Organic Electronics 14 (2013) 3123–3130

Contents lists available at ScienceDirect

Organic Electronics

journal homepage: www.elsevier.com/locate/orgel

Synergistic effects of buffer layer processing additives for enhanced hole carrier selectivity in inverted Organic Photovoltaics

Achilleas Savva [a], Marios Neophytou [a], Charalambos Koutsides [b], Kyriacos Kalli [b], Stelios A. Choulis [a,*]

[a] Molecular Electronics and Photonics Research Unit, Department of Mechanical Engineering and Materials Science and Engineering, Cyprus University of Technology, Kitiou Kiprianou str. 45, 3603 Limassol, Cyprus

[b] Nanophotonics Research Laboratory, Department of Electrical Engineering, Computer Engineering and Informatics, Cyprus University of Technology, Kitiou Kiprianou str. 45, 3603 Limassol, Cyprus

ARTICLE INFO

Article history:
Received 20 May 2013
Received in revised form 2 July 2013
Accepted 18 July 2013
Available online 2 August 2013

Keywords:
Inverted organic solar cells
Printed electronics
Solution based electronic materials
Interfaces
Processing additives
PEDOT:PSS buffer layers

ABSTRACT

Solution based inverted Organic Photovoltaic (OPVs) usually use Poly(3,4-ethylenedioxythiophene):poly(styrenesulfonate) (PEDOT:PSS) derivatives combined with pristine processing additives as hole selective contact on top of the hydrophobic conjugated polymer:fullerene active layer. In this study, PEDOT:PSS based hole selective contact is treated with two different boiling point additives, 2,5,8,11-tetramethyl-6-dodecyn-5,8-diol ethoxylate (Dynol) and Zonyl FS-300 fluorosurfactant (Zonyl). Although corresponding inverted OPVs using the above PEDOT:PSS:Additives show similar power conversion efficiency (PCE) values, the mechanisms of their implementation on inverted OPV operation are not identical. By understanding the synergistic effects of PEDOT:PSS processing additives on the hole selectivity of inverted OPVs we demonstrate a novel combination of PEDOT:PSS additives mixture as an effective route to further increase the hole selectivity, reliability andpower conversion efficiency of inverted OPVs.

1. Introduction

Over the last few years, the increased scientific interest in the field of Organic Photovoltaics (OPVs) resulted in power conversion efficiencies (PCE) near 10% [1]. In general three approaches have dominated the field of OPVs, single cell normal structured OPVs [2], single cell inverted OPVs [3] and tandem OPVs [4]. Up to today most of the published data are based on the normal device architecture. Tandem OPVs is a promising approach and already PCEs of over 10%, using either solution processed, polymer based [5], or vacuum processed, small molecule based devices [6] have been reported. Another exciting concept is the combination of more than two cells, one on the top of the other consecutively (multi-junction OPVs) [7], but still, a lot of progress needs to be done in the interconnecting layers between the cells [8], in order to meet the predictions for tandem OPVs with PCE near 15% for optimised material combinations [9].

Inverted bulk heterojunction solar cells could allow more flexibility on designing the roll-to-roll production process of OPVs and thus provide technological opportunities [10]. In addition, this interesting device architecture, allows studying fundamental processes in bulk heterojunction concept, including the vertical phase segregation of polymer/fullerene composites as well as the charge selectivity of the contacts [11]. In the inverted structure the electrons are extracted at the bottom electrode (ITO/n-type metal oxide) and the holes are extracted at the top electrode (Poly(3,4-ethylenedioxythiophene):poly(styrenesulfonate)(PEDOT:PSS)/Metal) [12]. Recent studies

* Corresponding author. Tel.: +357 25002605.
E-mail address: stelios.choulis@cut.ac.cy (S.A. Choulis).

1566-1199/$ - see front matter © 2013 Elsevier B.V. All rights reserved.
http://dx.doi.org/10.1016/j.orgel.2013.07.024

demonstrated inverted OPVs between 8% and 9% certified PCE, by using newly synthesized conjugated polymers and by incorporating novel buffer layers to form the top selective contact [13,14].

This remarkable progress, demonstrates the potential of OPVs to reach the PCEs of their silicon competitors, but still, a lot of issues have to be investigated in order to meet the requirements of a low cost, large scale production of OPVs. The employment of spin-coating techniques for the active layer and vacuum deposition processing of the hole selected top contact [13,14], are unfavorable for low cost printing processing. Recent reports, demonstrate inverted OPVs using solution based metal oxide hole selective contacts, with PCE comparable with those of inverted OPVs using PEDOT:PSS as the solution processed buffer layer of the top electrode [15,16].

Despite the recent progress, PEDOT:PSS is still the most common solution based hole selective contact in inverted OPVs top electrode, because of its tunable electronic properties and compatibility with various printing processes. Many reports have demonstrated that the incorporation of additives in PEDOT:PSS such us ethylene glycol [17], dimethyl sulfoxide (DMSO) [18], sorbitol [19,20], and glycerol [21], can result in increased conductivity. These high conductivity values (in some cases over 1000 S/cm) in combination with high transmittance in the visible portion of light, makes PEDOT:PSS a good candidate to efficiently used as ITO replacement [22,23], or as one of the two counterparts of the intermediate layer in tandem OPVs [24].

PEDOT:PSS water dispersions exhibit high surface tension because of their hydrophilic nature. The high surface tension of PEDOT:PSS is a major issue in the fabrication of inverted OPVs using solution based PEDOT:PSS as the selective top contact. Despite that the aforementioned additives, drastically enhance the electronic properties of PEDOT:PSS, are not able to reduce the surface tension of PEDOT:PSS solutions (Supporting info. Fig. S1). Based on that, processing additives used as wetting agents, such as isopropanol, have been incorporated in PEDOT:PSS, resulting in reduced surface tension and addressing the problem of wettability of PEDOT:PSS buffer layer, coated on top of hydrophobic polymer:fullerene active layers on the inverted OPV structure [10]. Despite the recent progress in the development of inverted solar cells using PEDOT:PSS:wetting agents/Metal top electrode, literature reports trying to investigate the effect of those wetting agents [25] on the inverted OPV device processing and operation are limited and thus it is still unclear how those wetting agents affect the hole selectivity of the inverted OPV top electrode.

In this study two different wetting agents have been used in PEDOT:PSS buffer layers, 2,5,8,11-tetramethyl-6-dodecyn-5,8-diol ethoxylate (Dynol 604) and Zonyl FS-300 fluorosurfactant (Zonyl). Both wetting agents have been used previously to overcome the poor wetting properties of PEDOT:PSS when coated on top of P3HT:PCBM blends [11,26,27]. We note that Dynol 604 is a non-ionic, non-fluorinated surfactant with boiling point ~340 °C, while Zonyl is a non-ionic fluorosurfactant with boiling point ~80 °C. The reason of choosing these two wetting agents among others, is the difference in their boiling points and their suitability with all commercially available types of PEDOT:PSS that we used. In contrast, we found that isopropanol cannot be used in all commercially available PEDOT:PSS solutions (Supporting info. Fig. S2).

Inverted OPVs with a range of concentrations of Zonyl and Dynol wetting agents in PEDOT:PSS, between 0.1 and 2 wt%, were fabricated (Supporting info. Fig. S3). The concentrations 0.2% and 0.5% for Dynol and Zonyl in PEDOT:PSS respectively were chosen based on the optimised inverted OPV device performance obtained for the above concentrations. The presented results focus on the optimised concentrations of Dynol, Zonyl and their mixture in PEDOT:PSS hole selective contact.

The device architectures studied are summarised as follows. Our control devices based on Zonyl treated PEDOT:PSS as hole selective contact (ITO/TiO_x/P3HT:PCBM/PEDOT:PSS:0.5 wt% Zonyl/Ag – "Z-device") are compared with device architectures that use Dynol treated PEDOT:PSS hole selective contact (ITO/TiO_x/P3HT:PCBM/PEDOT:PSS:0.2 wt% Dynol/Ag – "D-device"). Finally, both sets of devices are compared to solar cells with a mixture of Dynol and Zonyl treated PEDOT:PSS hole selective contact (ITO/TiO_x/P3HT:PCBM/PEDOT:PSS:0.2 wt% Dynol + 0.5 wt% Zonyl/Ag – "M-device") as demonstrated in Fig. 1.

The effect of the two pristine wetting agents, as well as, the proposed Dynol/Zonyl wetting agents mixture in PEDOT:PSS hole selective contact is analysed in terms of understanding the processing parameters and inverted OPV device principles. Contact angle measurements for wetting properties analysis, atomic force microscopy (AFM) based surface topography studies, external quantum efficiency (EQE) measurements, photocurrent plots and current density vs. voltage characteristics (J/V) under light and dark conditions, are introduced. The characteristics of PEDOT:PSS buffer layers, both in liquid and solid phase, proves that the interfacial properties of the PEDOT:PSS/Ag hole selective top electrode can be optimised by a suitable PEDOT:PSS wetting agents mixture. By understanding the mechanisms of the PEDOT:PSS wetting agents on the performance of inverted OPVs we show that the proposed mixture (Zonyl 0.5%:Dynol 0.2%), results in optimised hole selectivity, improved reliability and over 12% improvement on the PCE (mean and peak PCE values), compared with inverted OPVs using pristine PEDOT:PSS wetting agent as the selective top contact.

2. Experimental

The pre-sputtered glass-ITO substrates (Microliquid-sheet resistance 4 Ω/sq) were sonicated in acetone and subsequently in isopropanol for 10 min. The TiO_x precursor [tetra-n-butyl titanate, DuPont] was mixed with isopropanol and stirred for at least 30 min. The resulting solution was doctor bladed on top of ITO substrates and annealed for 30 min at 140 °C in ambient conditions. During the annealing process an amorphous layer of TiO_x of ~50 nm thickness was formed, as measured with a Veeco Dektak 150 profilometer. The photo-active layer, a blend of P3HT:PCBM (1:0.8 wt%) in chlorobenzene, was doctor bladed on top of TiO_x resulting in a thickness of

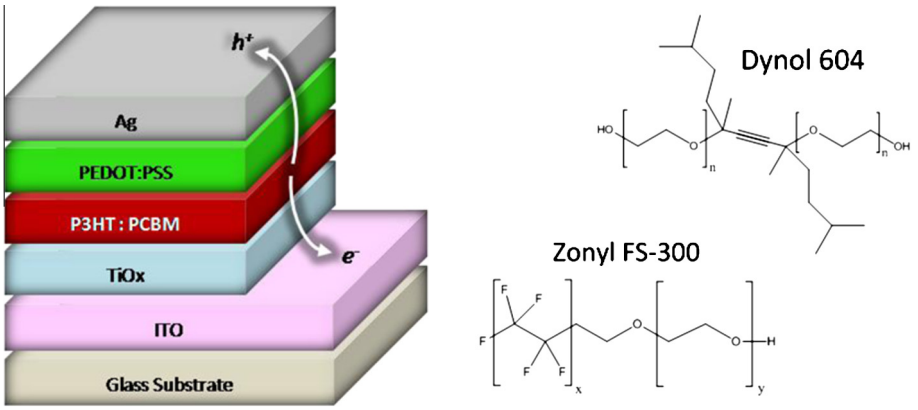

Fig. 1. Schematic of the inverted OPV structure used in the reported studies, ITO/TiO_x/P3HT:PCBM/PEDOT:PSS:Additive (Dynol/Zonyl or Dynol + Zonyl mixture)/Ag, and the chemical structures of the pristine PEDOT:PSS additives Dynol and Zonyl.

~230 nm. The hole selective layer used in this study is PEDOT:PSS Clevios PH (HC Stark). The two surfactants Zonyl FS-300 (Sigma Aldrich) and Dynol 604 (Air Products and Chemicals Inc.) were added to PEDOT:PSS PH and stirred vigorously for 15 min before deposition. During the doctor blading deposition the blade speed, volume and blade height was kept constant for all the devices, resulting in a PEDOT:PSS PH thickness of 70 nm in all cases. The devices were annealed inside a glovebox at 140 °C for 22 min and after that a silver layer with a thickness of 100 nm was thermally evaporated on top of PEDOT:PSS PH. On each ITO substrate there are four devices with active area 0.09 mm^2, which is accurately defined by the evaporation mask.

Contact angle measurements have been performed using a KRUSS DSA 100E drop analysis system. For the surface energy measurements, the contact angle of water, diiodomethane and ethylene glycol was measured, on top of P3HT:PCBM layer. The processing conditions for the P3HT:PCBM surface energy measurements is identical to device processing steps used for the inverted OPVs presented within the manuscript. Based on these results, the software derived the polar and dispersive parts of the surface energy of the solids and hence the wetting envelopes using the "OWRK" method [12]. The polar and dispersive parts of the surface tension of the liquids were calculated via the pendant drop method, using the interfacial surface tension between the liquids and the air and the contact angle of each liquid on a standard Teflon surface.

The current density–voltage (J/V) characteristics were measured with a Keithley source measurement unit (SMU 2420). For illumination a calibrated Newport Solar simulator equipped with a Xe lamp was used, providing an AM1.5G spectrum at 100 mW/cm^2. EQE measurements were carried out on a setup comprising a Xe lamp, a monochromator, a current–voltage preamplifier and a lock-in amplifier.

AFM measurements have been applied on the samples in order high resolution images to be extracted. As cantilever is much harder than coatings, we avoid applied contact mode measurements as the pin could scratch the surface. For that reason tapping mode AFM measurements have been applied and both height and phase images have been extracted A Veeco setup has been used for these measurements.

3. Results and discussion

3.1. The effect of additives on the wetting properties of PEDOT:PSS

As mentioned previously a major issue in the processing of inverted OPVs is the poor wetting properties of water based PEDOT:PSS on the surface of the hydrophobic P3HT:PCBM active layer. This problem is addressed by the use of surfactants as additives, which tend to reduce the surface tension of water. Fig. 2 demonstrates the contact angle measurements performed to investigate this effect. Detailed description about wetting envelopes and surface tension calculations are described elsewhere [12].

Fig. 2a demonstrates the surface tension of four different types of commercially available PEDOT:PSS solutions and the wetting envelope of P3HT:PCBM layer. Although the different types of PEDOT:PSS vary in properties, such us conductivity and PSS content, the surface tension has been found to be similar in the 4 compared PEDOT:PSS types. Al4083 (conductivity 0.002 S/cm), PH (10 S/cm), PH500 (500 S/cm), PH1000 (800 S/cm) surface tensions, have found to be: 68.55 mN/m, 69.39 mN/m, 66.59 mN/m, 67.61 mN/m, respectively. Compared to the other four types, PEDOT:PSS JET NV2 (neutral 5–8 pH, 700 S/cm) exhibits reduced surface tension at 37 mN/m. Neutral and highly conductive PEDOT:PSS are favourable for the tandem cell recombination layer[7]. Despite the reduce surface tension of NV2, all types of PEDOT:PSS, which are the most commonly used in OPVs, exhibit surface tensions that lie well outside the wetting envelope of P3HT:PCBM, which is a proof of the poor layer formation of different types of PEDOT:PSS on top of the hydrophobic P3HT:PCBM active layer. When 0.5% of Zonyl was added to the water dispersion of PEDOT:PSS PH the surface tension was reduced to 19.13 mN/m. Similar effect has been observed when 0.2% Dynol was added in PEDOT:PSS PH solution and resulted to a surface tension of 21.04 mN/m (Fig. 2b). The surface tension was further reduced (17.12 mN/m)

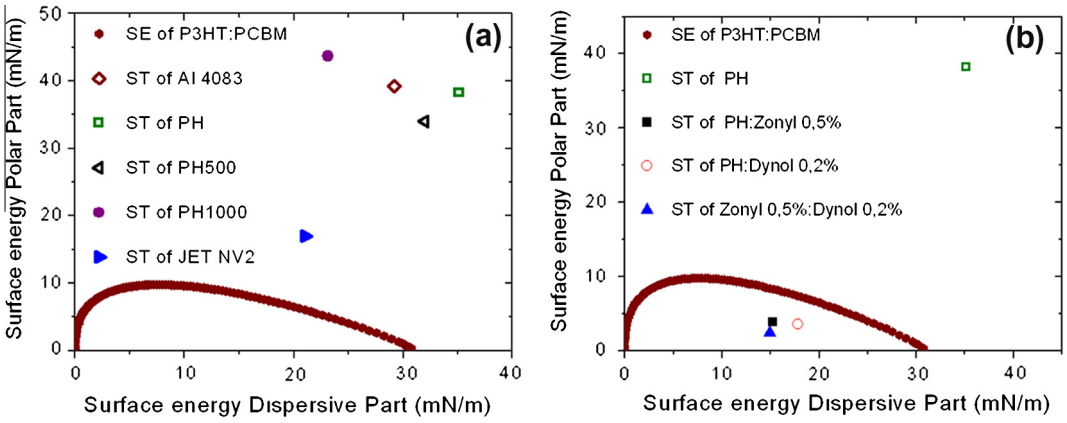

Fig. 2. (a) Surface energy (SE) wetting envelope of P3HT:PCBM layer (closed polygons) and surface tensions (ST) of various commercially available PEDOT:PSS solutions (used as received) with different chemical and electronic properties. (b) Surface energy wetting envelope of P3HT:PCBM layer (closed polygons), surface tension of PEDOT:PSS PH (open square) surface tension of PEDOT:PSS:Zonyl 0.5% (filled squares), surface tension of PEDOT:PSS:Dynol 0.2% (open circles) and surface tension of PEDOT:PSS:Zonyl 0.5%:Dynol 0.2% (filled triangles). The inserts represent the contact angle on a standard Teflon surface (left) and the pendant drop in air (right) for the respective PEDOT:PSS solution.

when the proposed combination of 0.5% Zonyl and 0.2% Dynol was used as an additive in PEDOT:PSS solution. The pictures in Fig. 2 depict the dropletshape in air for all PEDOT:PSS solutions under study and the contact angles of the liquids on a standard TEFLON surface, which were found to be 95°, 39°, 42°, 21° for the pristine PEDOT:PSS, PEDOT:PSS:0.5% Zonyl, PEDOT:PSS:0.2% Dynol and PEDOT:PSS:0.5% Zonyl:0.2% Dynol, respectively. The results reported prove that the reduced surface tension caused by addition of additives in PEDOT:PSS can address the issue of processing and thus homogeneous PEDOT:PSS buffer layers on top of the hydrophobic P3HT:PCBM active layer suitable for inverted OPV operation can be obtained. Similar results has been observed for all the types of PEDOT:PSS reported in Fig. 2a (data not shown). Based on our measurements we concluded that Dynol is a better wetting agent than Zonyl, due to the lower additive concentration needed to achieve suitable reduction in surface tension of PEDOT:PSS. However for all the proposed additives the wetting issues of PEDOT:PSScan be eliminated with the use of small quantities of surfactants and allow the fabrication of efficient inverted OPVs with PEDOT:PSS/Ag as hole selective top electrode in good agreement with previous published device performance data [10,11].

3.2. The effect of additives on hole selectivity and device performance of inverted OPVs

Fig. 3a and b shows representative dark and illuminated *J*/*V* characteristics of the three inverted OPVs under study, as schematically depicted in Fig. 1. Our control devices based on Zonyl treated PEDOT:PSS buffer layer (ITO/TiO_x/P3HT:PCBM/PEDOT:PSS:0.5 wt% Zonyl/Ag – "Z-device") are compared with device architectures that use Dynol treated PEDOT:PSS buffer layer (ITO/TiO_x/P3HT:PCBM/PEDOT:PSS:0.2 wt% Dynol/Ag – "D-device"). Finally, both sets of devices are compared to solar cells with a mixture of Dynol and Zonyl treated PEDOT:PSS buffer layer (ITO/TiO_x/P3HT:PCBM/PEDOT:PSS:0.2 wt% Dynol + 0.5 wt% Zonyl/Ag – "M-device"). Each *J*/*V* curve is a representative device curve out of 12 devices for each case produced in the same experimental run. In total over 100 devices were fabricated showing reproducible and high reliable device performance.

The illuminated *J*/*V* characteristics (Fig. 3a) show identical open circuit voltage (V_{oc}): 0.57 V for M, D and Z-device and similar short circuit current density (J_{sc}) values: M-device 9.61 mA/cm^2, D-device 9.31 mA/cm^2 and Z-device 9.26 mA/cm^2. Despite that, Fig. 3a in combination with the dark *J*/*V* characteristics (Fig. 3b) demonstrate that D-device shows better behaviour at high positive voltage (series resistance – R_s) but on the other hand, increased leakage current at high negative bias (R_p) compared to Z-device. This is a proof that, despite that Z- and D-device results in similar power conversion efficiency (PCE – 3.24% and 3.11% respectively) the two compared inverted OPVs have different behaviour in the R_s and R_p regions. Based on the above observations, the new proposed mixture of 0.5% Zonyl and 0.2% Dynol in PEDOT:PSS (M-device) has been investigated in detail under this study. The results prove better charge carrier selectivity (highest injection current, R_s, and low leakage current, R_p) for the M-device compared to Z- and D-device and thus improved FF (M-device 64%, D-device 61% and Z-device 60%) and 12% improved PCE (3.55%). The values of R_s and R_p for all the representative diodes under study, have been calculated using a simulation model described previously by Waldauf et al. [28].

Series resistance is one of the most important parameters of organic diodes operation and arises from the resistance of the contacts to the current flow, particularly at the interfaces between the active layer and the electrodes [29]. It is has been reported that sheet resistance (R_{sheet}) of the electrodes has an influence in R_s of an organic diode [30,31]. From Fig. 3a and b we observe that R_s is smaller for the M-device compared to D- and Z-device. Since the contacts between ITO/TiO_x/P3HT:PCBM are the same for all the inverted OPVs under investigation we conclude that

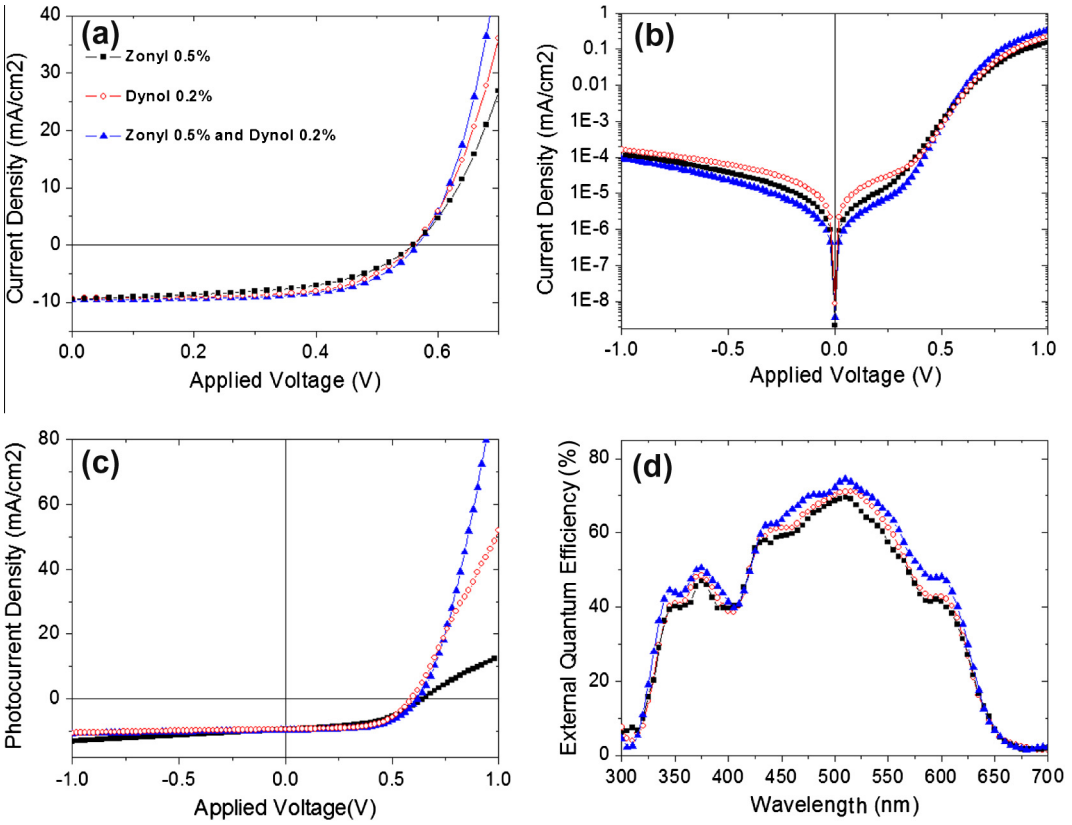

Fig. 3. (a) Illuminated *J*/*V* characteristics for inverted organic solar cells using PEDOT:PSS:0.5% Zonyl (filled squares), PEDOT:PSS:0.2% Dynol (open circles) and PEDOT:PSS:0.5% Zonyl:0.2% Dynol (filled triangles). (b) Dark *J*/*V* characteristics, (c) photo-current density vs. voltage characteristics and (d) external quantum efficiency for the aforementioned diodes.

the reduced R_s observed for the M-device possibly originates from the reduced sheet resistance of PEDOT:PSS:0.2% Dynol:0.5% Zonyl hole selective contact due to increased conductivity. This assumption is related with our morphological observation of the films treated with different wetting agents and are presented in Fig. 5.

Photocurrent–voltage measurements (Fig. 2c) of the inverted OPVs under study were used to further investigate the effect of PEDOT:PSS additives on the performance of inverted OPVs. Fig. 3c shows the measured photocurrent as a function of diode bias for the three inverted OPVs under study. Photocurrent measurements can be used to measure the built-in potential (V_{bi}) and thus the changes in the energy barriers at the interfaces between the active layer and the electrodes [32]. The V_{bi} was found to be 0.62 V, 0.60 V and 0.64 V for the M-device, D-device and Z-device respectively. The results do not indicate any change in V_{bi} since the difference of 0.02 V for the compared diodes is within the experimental error. Based on these results, the treatment of the PEDOT:PSS with the different additives is unlikely to alter the electronic properties of the inverted OPVs top electrode.

External quantum efficiency (EQE) measurements (Fig. 3d) represent the percentage of the photons escaping the source, which are collected as electrons by the terminals of the device for a selected wavelength range. Detailed analysis of EQE measurements are described elsewhere [33]. Fig. 3d indicates that D-device shows slightly better EQE than the Z-device, while the M-device exhibits higher EQE compared to the other two in agreement with the *J*/*V* plots reported before (Fig. 1a). To confirm the accuracy of our measurements we calculated the theoretical current density (J_{sc}) by multiplying the EQE by the AM1.5G spectrum and integrating the result. The small mismatch (5.3% maximum) between experimental and theoretical J_{sc} indicates high accuracy measurements. Table 1 summarise the results and calculations for the three inverted OPVs under study extracted from illuminated and dark *J*/*V* characteristics, photocurrent and EQE measurements.

Box plots of Fig. 4 summarise the performance parameters of the inverted OPVs under study. Three series of cells with 12 devices each were investigated. We note that the data presented here have been collected from the same experimental run but were confirmed and reproduced in several other independent runs. The box plots of Fig. 4 indicate high reproducibility for all the series of solar cells reported and this is a result of the detailed optimisation process performed for all the inverted OPVs under study. In consistency with our previous comments, Fig. 4a and b indicates that the inverted OPVs under comparison have similar V_{oc} and J_{sc}. On the other hand, over 60% of M-devices exhibit superior FF values compared to D- and Z-devices, indicating the improved hole selectivity achieved by the new proposed PEDOT:PSS wetting agents mixture.

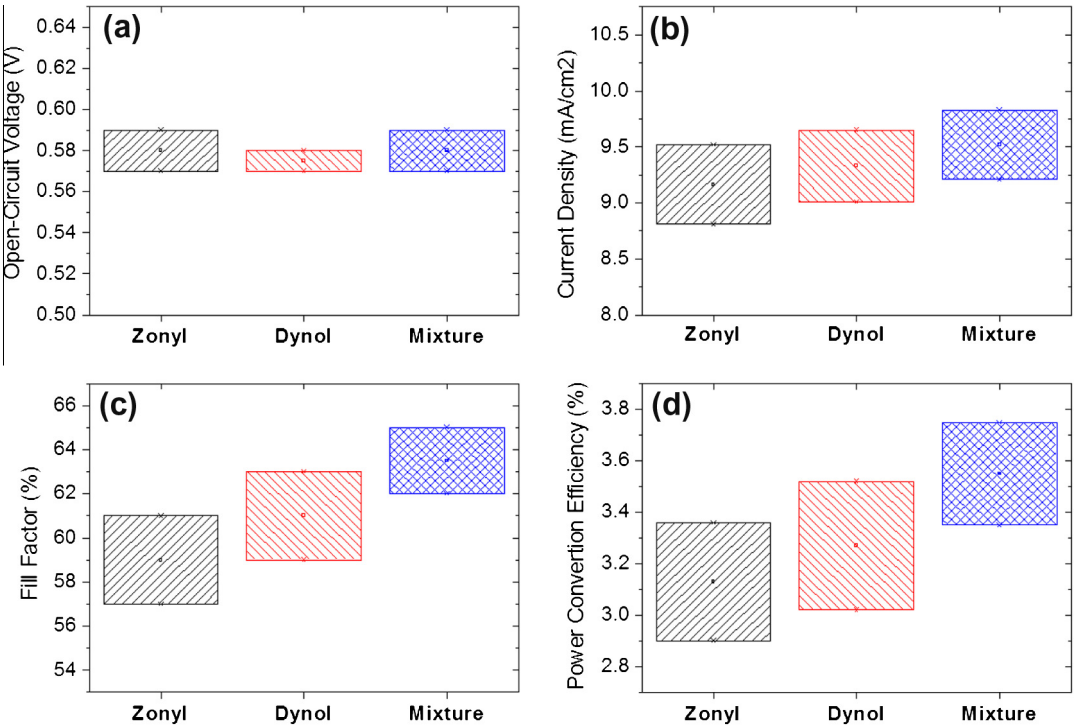

Fig. 4. Comparison of the (a) open circuit voltage (V_{oc}), (b) short circuit current density (J_{sc}), (c) fill factor (FF), and (d) power conversion efficiency (PCE) for the solar cells under study.

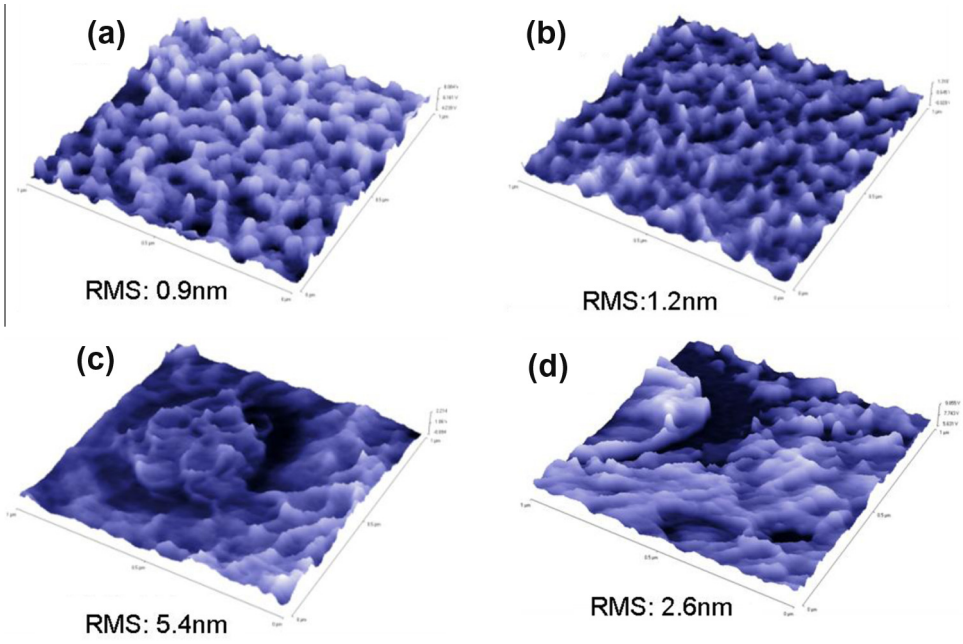

Fig. 5. Tapping mode (1 μm × 1 μm) AFM measurements. Phase 3D images of (a) pristine PEDOT:PSS PH, (b) PEDOT:PSS:0.5% Zonyl, (c) PEDOT:PSS:0.2% Dynol and (d) PEDOT:PSS:0.2% Dynol:0.5% Zonyl.

Regarding the PCE values we observe that the D-devices and Z-devices have rather similar performance, and only a percentage of 25% of D-devices have slightly better PCE values than the Z-devices. In contrast, Z-devices seem to have better reproducibility than D-devices. Finally, over 50% of M-devices (using the new proposed PEDOT:PSS

Table 1
Summary of the experimental and theoretical values for the compared devices.

Device	V_{oc} (V)	J_{sc} (mA/cm^2)[a]	FF (%)	PCE (%)[b]	R_p (Ω cm^2)	R_s (Ω cm^2)	V_{bi} (V)
Z-device	0.57	9.26(8.77)	60	3.11(3.36)	5481	5.32	0.64
D-device	0.57	9.31(9.02)	61	3.24(3.42)	4812	3.19	0.60
M-device	0.57	9.61(9.65)	64	3.55(3.75)	6327	1.81	0.62

[a] In brackets the theoretical values of J_{sc}.
[b] Average values of PCE after evaluation of over 100 devices. In brackets the maximum values of PCE.

additive mixture) have a PCE over 3.5%, which is better than the PCE values obtained for D-devices and Z-devices (using pristine PEDOT:PSS additives) combined with better reproducibility performance. Importantly the proposed additive mixture can be applied in other types of PEDOT:PSS derivatives and can also be used in combination with other additives such as ethylene glycol (EG) (see Supporting information Fig. S4). Fig. S4b (Supporting information) demonstrates inverted OPVs optimum device performance and diode behaviour (PCE over 4%) when PEDOT-PH500 is treated with Zonyl/Dynol mixture 0.7% and EG 5% to form the hole selective contact.

3.3. The effect of additives on PEDOT:PSS surface topography

In order to examine the surface topography of PEDOT:PSS buffer layers treated with different processing additives, atomic force microscopy (AFM) studies were performed. Pristine PEDOT:PSS solution was coated on glass because it was unable to be coated on top of the active layer due to the poor wetting properties of PEDOT:PSS on top of P3HT:PCBM. All the other samples were fabricated identically with the layers used for the representative inverted OPV device structures presented in Fig. 3 and annealed at 140 °C for 30 min before examination.

Fig. 5a, demonstrates the AFM measurement for a pristine PEDOT:PSS buffer layer. The image of PEDOT:PSS films, in where the bright (positive) and dark (negative) phase shifts correspond to PEDOT-rich grains and PSS-rich grains respectively, is in good agreement with the literatures [18,34] and the surface roughness of this film was found to be 0.9 nm. Fig. 5b (PEDOT:PSS:0.5% Zonyl) indicates a slightly different morphology compared to the pristine PEDOT:PSS films with rougher and more aggregate surface at 1.2 nm. Fig. 5c demonstrates the AFM image of PEDOT:PSS:0.2% Dynol films. We observe different surface topography compared to the other two films with discontinuity in the networks of PEDOT and PSS grains. Despite that the average roughness measurement for 1 μm^2 was 5.4 nm the film looks smoother in particular areas (3.4 nm) and rougher to other areas in where we observe the formation of clusters (6.6 nm). We note here that Fig. 5c was a representative image of the PEDOT:PSS:0.2% Dynol films and several other images of PEDOT:PSS layers treated with 0.2% Dynol reveal the same cluster formation. Fig. 5d demonstrates a representative AFM measurement of PEDOT:PSS:0.5% Zonyl:0.2% Dynol mixture. The surface topography observed is closer to the morphology observed for PEDOT:PSS treaded with Dynol and reveals again the inhomogeneities on the surface. Despite that, the surface roughness of the overall area (1 μm^2) was found to be 2.6 nm, the smoother areas 1.3 nm and the cluster areas 3.4 nm. The difference in morphology between PEDOT:PSS:0.5% Zonyl and PEDOT:PSS:0.2% Dynol films is attributed to the different boiling points of the two wetting agents. The evaporation rate of Zonyl is higher (b.p. $\sim$ 80 °C) than Dynol (b.p. $\sim$ 320 °C) during the annealing process of PEDOT:PSS causing different ordering within the material and different PEDOT and PSS network arrangement. This different orientation of PEDOT and PSS chains observed for PEDOT:PSS:0.2% Dynol and PEDOT:PSS:0.7% mixture compared to PEDOT:PSS:0.5% Zonyl, seems to be beneficial for inverted OPVs operation, since inverted OPVs using Dynol or mixture treated PEDOT:PSS exhibit reduced R_s and better FF than inverted OPVs using Zonyl treated PEDOT:PSS hole selective contacts (Fig 3a and b). The effect of pristine Zonyl in PEDOT:PSS is mainly on the better leakage current observed for the corresponding inverted OPVs, effect which is also evident in the inverted OPV device performance when a mixture of Zonyl:Dynol in PEDOT:PSS is used. It has been shown that morphological and surface topography modifications of PEDOT:PSS with additives can affect the PEDOT:PSS conductivity values [26].

4. Conclusions

In summary, we presented a detailed study on the role of PEDOT:PSS wetting agents on the device performance of inverted OPVs. We have probed the influence of Zonyl, Dynol and their optimise mixture on the wetting, electronic and surface properties of PEDOT:PSS buffer layers. Various PEDOT:PSS derivatives ranging in electrical conductivity properties cannot be used as received to fabricate inverted OPVs because of the poor wetting properties of the solutions on top of the hydrophobic active layer. The use of both of the pristine wetting agents assisted to overcome this issue and thus PEDOT:PSS can be used in highly efficient OPV devices with inverted layer sequence. Although the processing treatment of PEDOT:PSS buffer layer with the different additives is unlikely to alter the electronic properties of the top electrode the surface topography studies presented revealed altered morphology due to differences in the additives boiling points. By understanding the mechanisms of the PEDOT:PSS wetting agents on the performance of inverted OPVs we have proposed a PEDOT:PSS wetting agent mixture of (Zonyl:Dynol) as an effective route to further increase the hole selectivity of inverted OPVs top electrode. The best inverted OPV device performance (higher FF and PCE) achieved when a

combination of Dynol:Zonyl is used in PEDOT:PSS buffer layer, as demonstrated in *J*/*V* analysis under illumination. The improved FF is a result of the reduced series resistance and leakage current observed in the inverted OPVs when PEDOT:PSS hole selective contact was treated with the combination of the proposed additive mixture. The proposed additive mixture of (Zonyl 0.5%:Dynol 0.2%) results in improved reliability and 12% improvement on the PCE of solution based inverted OPVs.

Acknowledgements

This work was co-funded by the European Regional Development Fund and the Republic of Cyprus through the Research Promotion Foundation (Strategic Infrastructure Project NEA ΥΠΟΔΟΜΗ/ΣΤΡΑΤΗ/0308/06). A.S. would like to thank Air Products and Chemicals Inc. for providing a free sample of Dynol 604. Furthermore A.S., C.K. and K.K. would like to thank Graham Lee for his help on AFM measurements.

Appendix A. Supplementary material

Supplementary data associated with this article can be found, in the online version, at http://dx.doi.org/10.1016/j.orgel.2013.07.024.

References

[1] M.A. Green, K. Emery, Y. Hishikawa, W. Warta, Solar cell efficiency tables (version 39), Prog. Photovolt.: Res. Appl. 20 (2012) 12–20.
[2] J.Y. Kim, S.H. Kim, H.H. Lee, K. Lee, W. Ma, X. Gong, A.J. Heeger, New architecture for high-efficiency polymer photovoltaic cells using solution-based titanium oxide as an optical spacer, Adv. Mater. 18 (2006) 572–576.
[3] C. Waldauf, M. Morana, P. Denk, P. Schilinsky, K. Coakley, S.A. Choulis, C.J. Brabec, Highly efficient inverted organic photovoltaics using solution based titanium oxide as electron selective contact, Appl. Phys. Lett. 89 (2006) 233517–233520.
[4] J. Gilot, M.M. Wienk, R.A.J. Janssen, Optimizing polymer tandem solar cells, Adv. Energy Mater. 22 (2010) 67–71.
[5] J. You, L. Dou, K. Yoshimura, T. Kato, K. Ohya, T. Moriarty, K. Emery, C.-C. Chen, J. Gao, Gang Li, Y. Yang, A polymer tandem solar cell with 10.6% power conversion efficiency, Nat. Commun. 4 (2012) 1446–1456.
[6] Heliatek. Heliatek Sets New World Record Efficiency of 10.7% for its Organic Tandem Cell. 2012. <http://www.heliatek.com/wp-content/uploads/2012/04/120427_PI_Heliatek-world-record-10_7-percentefficiency.pdf> (accessed 01.03.12).
[7] J. Gilot, M.M. Wienk, R.A. Janssen, Double and triple junction polymer solar cells processed from solution, Appl. Phys. Lett. 90 (2007) 143512–143515.
[8] N. Li, T. Stubhan, D. Baran, J. Min, H. Wang, T. Ameri, C.J. Brabec, Design of the solution-processed intermediate layer by engineering for inverted organic multi junction solar cells, Adv. Energy Mater. 3 (2013) 301–307.
[9] T. Ameri, G. Dennler, C. Lungenschmied, C.J. Brabec, Organic tandem solar cells: a review, Energy Environ. Sci. 2 (2009) 347–363.
[10] M.M. Voigt, R.C.I. Mackenzie, C.P. Yau, P. Atienzar, J. Dane, P.E. Keivanidis, D.D.C. Bradley, J. Nelson, Gravure printing for three subsequent solar cell layers of inverted structures on flexible substrates, Sol. Energy Mater. Sol. C 95 (2011) 731–734.
[11] R. Steim, S.A. Choulis, P. Schilinsky, C.J. Brabec, Interface modification for higly efficient organic photovoltaics, Appl. Phys. Lett. 92 (2008) 093303–093306.
[12] .A. Savva, F. Petraki, P. Elefteriou, L. Sygellou, M. Voigt, M. Giannouli, S. Kennou, J. Nelson, D.D.C. Bradley, C.J. Brabec, S.A. Choulis, The effect of organic and metal oxide interfacial layers on the performance of inverted organic photovoltaics, Adv. Energy Mater. 3 (2012) 391–398.
[13] Z. He, C. Zhong, S. Su, M. Xu, H. Wu, Y. Cao, Enhanced power-conversion efficiency in polymer solar cells using an inverted device structure, Nat. Photonics 6 (2012) 591–595.
[14] C.E. Small, S. Chen, J. Subbiah, C.M. Amb, S.W. Tsang, T.H. Lai, J.R. Reynolds, F. So, High-efficiency inverted dithienogermole–thienopyrrolodione-based polymer solar cells, Nat. Photonics 6 (2012) 115–120.
[15] C.-P. Chen, Y.-D. Chen, S.-C. Chuang, High-performance and highly durable inverted organic photovoltaics embedding solution-processable vanadium oxides as an interfacial hole-transporting layer, Adv. Mater. 23 (2011) 3859–3863.
[16] T. Stubhan, N. Li, N.A. Luechinger, S.C. Halim, G.J. Matt, C.J. Brabec, High fill factor polymer solar cells incorporating a low temperature solution processed WO_3 hole extraction layer, Adv. Energy Mater. 2 (2012) 1433–1438.
[17] Z. Hu, J. Zhang, Z. Hao, Y. Zhao, Influence of doped PEDOT:PSS on the performance of polymer solar cells, Sol. Energy Mater. Sol. C 95 (2011) 2763–2767.
[18] G.F. Wang, X.M. Tao, J.H. Xin, B. Fei, Modification of conductive polymer for polymeric anodes of flexible organic light-emitting diodes, Nanoscale Res. Lett. 4 (2009) 613–617.
[19] A.M. Nardes, R.A.J. Janssen, M. Kemerink, A morphological model for the solvent-enhanced conductivity of PEDOT:PSS thin films, Adv. Funct. Mater. 18 (2008) 865–871.
[20] A.M. Nardes, M. Kemerink, M.M. de Kok, E. Vinken, K. Maturova, R.A.J. Janssen, Conductivity, work function, and environmental stability of PEDOT:PSS thin films treated with sorbitol, Org. Electron. 9 (2008) 727–734.
[21] J. Huang, P.F. Miller, J.S. Wilson, A. de Mello, J. de Mello, D.D.C. Bradley, Adv. Funct. Mater. 15 (2009) 290.
[22] S.I. Na, G. Wang, S.S. Kim, T.W. Kim, S.H. Oh, B.K. Yu, T. Lee, D.Y. Kim, Evolution of nanomorphology and anisotropic conductivity in solvent-modified PEDOT:PSS films for polymeric anodes of polymer solar cells, J. Mater. Chem. 19 (2009) 9045–9053.
[23] Y.H. Kim, C. Sachse, M.L. Machala, C. May, L. Müller-Meskamp, K. Leo, Highly conductive PEDOT:PSS electrode with optimized solvent and thermal post-treatment for ITO-free organic solar cells, Adv. Funct. Mater. 21 (2011) 1076–1081.
[24] J. Yang, R. Zhu, Z. Hong, Y. He, A. Kumar, Y. Li, Y. Yang, A robust inter-connecting layer for achieving high performance tandem polymer solar cells, Adv. Mater. 23 (2011) 3465–3470.
[25] F.J. Lim, K. Ananthanarayanan, J. Luther, G.W. Ho, Influence of a novel fluorosurfactant modified PEDOT:PSS hole transport layer on the performance of inverted organic solar cells, J. Mater. Chem. 22 (2012) 25057–25064.
[26] M. Vosgueritchian, D.J. Lipomi, Z. Bao, Highly conductive and transparent PEDOT:PSS films with a fluorosurfactant for stretchable and flexible transparent electrodes, Adv. Funct. Mater. 22 (2012) 421–428.
[27] M. Glatthaar, M. Niggemann, B. Zimmermann, P. Lewer, M. Riede, A. Hinsch, J. Luther, Organic solar cells using inverted layer sequence, Thin Solid Films 491 (2005) 298–300.
[28] C. Waldauf, P. Schilinsky, J. Hauch, C.J. Brabec, Material and device concepts for organic photovoltaics: towards competitive efficiencies, Thin Solid Films 451 (2004) 503–507.
[29] J. Nelson, in: The Physics of Solar Cells, Imperial Collage Press, London, United Kingdom, 2002 (Chapter 1).
[30] C. Waldauf, M.C. Scharber, P. Schilinsky, J.A. Hauch, C.J. Brabec, Physics of organic bulk heterojunction devices for photovoltaic applications, J. Appl. Phys. 99 (2006) 104503–104509.
[31] P. Schilinsky, C. Waldauf, J. Hauch, C.J. Brabec, Simulation of light intensity dependent current characteristics of polymer solar cells, J. Appl. Phys. 95 (2004) 2816–2819.
[32] S.A. Choulis, V.E. Choong, A. Patwardhan, M.K. Mathai, F. So, Interface modification to improve hole-injection properties in organic electronic devices, Adv. Funct. Mater. 16 (2006) 1075–1080.
[33] G. Dennler, K. Forberich, M.C. Scharber, C.J. Brabec, I. Tomiš, Angle dependence of external and internal quantum efficiencies in bulk heterojunction organic solar cells, J. Appl. Phys. 102 (2007) 054516–054523.
[34] U. Lang, E. Müller, N. Naujoks, J. Dual, Microscopical investigations of PEDOT:PSS thin films, Adv. Funct. Mater. 19 (2009) 1215–1220.